A study of star-forming galaxies at 2.1 < z < 2.5 selected by broad-band flux excesses

Y.Terao, 2019 Doctoral Dissertation

Presenter: N.Chen

- Structure:
  - Abstract (2)
  - Introduction (4)
  - Data and Method (6)
  - Properties of Hα emitters at z = 2.1–2.5 (12)
  - Properties of [OIII] emitters at z = 2.1–2.5 (6)

Abstract

- **Target selection:**
- **“Flux Excess”:** a difference between an observed flux and a continuum flux from SED

  ZFOURGE database (wide wavelength coverage)
  SED fitting with the emission line templates
  → Accurate continuum flux levels (SED)

  → Hα-emitters (K_s-band) and [OIII] emitters (H_s/H_l-band) at 2.1 < z < 2.5

- Comparing “flux excess” with narrow-band color excesses, long-slit spectroscopy and integral-field spectroscopy

  → Accuracy (fluxes within a factor of 2) 73%, 67% and 62%

  → no significant error introduced by using the flux excess

- **Properties:**

  UVJ diagram —— works properly to select the star-forming galaxies

  - **Strong [Hα] emitters:**
  - 1. Correlation between SFRs and dust attenuation to Hα (luminous ↑, dusty ↑)
  - 2. Hα LF:

    This paper ↔ High-z Emission Line Survey (HiZELS), An excess in the bright-end
    - a. extended Hα profiles (different size of aperture) b. dust attenuation
  - 3. The star formation main sequence (SFMS) of Hα-emitters
    - Agrees well with previous studies at $logM/M_{\odot} > 9$
    - Much more low-mass galaxies above SFMS (large Hα/UV ratios → starburst)

  - **Strong [OIII] emitters:**

    large sSFRs, large [OIII]λ5007/Hβ ratios, small dust attenuation, a sub-population of the Hα-emitters

Introduction

- 1.1 Galaxy evolution through cosmic time
  - 1.1.1 Cosmic star formation rate density: the history of the stellar mass assembly
    - The cosmic SFRD has a peak at ~ 10–11 Gyr ago (z ~ 2–3)
  - 1.1.2 SFMS: the correlation between stellar masses and SFRs of galaxies

$$\log SFR = a \log M + b, \qquad \text{a = (0, 1), b increases toward high-z}$$

    - → more active star formation of galaxies in the early universe than today (20 times for z ~ 2)
    - The scatter around the SFMS (~ 0.3 dex): "self-regulated" process (Tacchella et al. (2016))
      → Star formation is governed by gas inflows and depletions
    - The low mass end of SFMS ($logM/M_{\odot}$ < 9): show larger scatters around the SFMS than massive ones (Sparre et al.(2017))
      → Stronger SN feedback and starburst (~ 10 Myr)
    - Finding galaxies with busty SFHs → the luminosity ratios of Hα and UV (~ 100 Myr for UV)

- 1.1.3 Equivalent width
  - Equivalent widths become higher with increasing redshift (Fumagalli et al. (2012))
  - Higher equivalent widths show lower stellar masses, younger ages, and higher sSFRs, **ionization parameters and ionizing photon production efficiencies**. (Most significant to the [OIII]) (Reddy et al. (2018))
  - → galaxies with high [OIII] equivalent widths may enable us to understand populations which contribute to the cosmic re-ionization

- 1.2 Selection of star-forming galaxies (features in their spectra)
  - 1.2.1 Nebula emission lines
    - Originated from nebulae ionized by radiations of young stars: Lyα, Hα, [OII] and [OIII]
  - 1.2.2 Lyman break (UV easily absorption by dust → less dusty systems (e.g., Oteo et al. 2015))
  - 1.2.3 UVJ diagram
    - The bimodality of the star-forming and the quiescent populations on the UVJ diagram persists at least up to $z \sim 2.5$ (Williams et al. 2009, Whitaker et al. 2011)
      - The (U−V) colors of the quiescent galaxies become bluer with increasing redshift, while their (V−J) colors do not change.
      - The number fraction of the dusty star-forming galaxies increases toward high-z.
      - High-z dusty star-forming galaxies have redder (V−J) colors than those at lower redshift

- 1.3 SFR indicators
  - 1.3.1 UV continuum
    - UV continua between 1216–3000 Å (from stars with mass > 5 $M_{\odot}$, lifetime ~ 100 Myr)
    - Easily absorbed by interstellar dust
  - 1.3.2 Hα emission line
    - The ionizing photons are produced by the most massive stars(> 10 M⊙, lifetime ~ 10 Myr)
    - → nearly instantaneous star formation, still need to take the dust attenuation into account
  - 1.3.3 [OII]λλ3726, 3729 doublet
    - [OII] luminosities generally correlate with Hα luminosities, but the [OII] SFRs are more uncertain.

- 1.4 Observation types
  - 1.4.1 Imaging
    - Advantage: observing many galaxies at once in the FOVs, obtain spatial information and morphology.
    - Disadvantage:
    - Broad-band: When fitting SED, precise information on spectra such as the emission lines are lost
    - Narrow-band: Need much time than the broad-band imaging surveys
  - 1.4.2 Spectroscopy
    - Using slit masks which are designed by aligning one or several long slits on the target objects
    - Advantage: accurate measurements Disadvantage: miss lights from out-skirts, longer time

- 1.5 Aim of this thesis
  - Verifying a method to derive emission line (Hα emitters and [OIII] emitters) fluxes from broad-/medium-band photometry at z = 2.1–2.5 using a multi-band photometry catalog of ZFOURGE.
  - Investigating properties of the Hα and [OIII] emitters at $2.1 < z < 2.5$

Data and Method

- 2.1 ZFOURGE catalog
  - 80% completeness has been achieved for galaxies with logM ~ 9.0 at z = 2.
  - ZFOURGE: medium-band filters J_1, J_2, J_3 and H_S, H_I

Table 2.1: Summary of ZFOURGE catalog

field	COSMOS	UDS	CDFS
area (arcmin^2)	139.2	135.6	132.2
Ks depth (AB mag,5σ)	25.5	25.7	26.2–26.5
# of filter	38	27	43
coverage (μm)	0.8–8, 24	0.8–8, 24	0.8–8, 24, 100, 160
σ_z	0.022	0.013	0.020

- 2.2 Emitter selection by flux excess

  "Flux excess" (in units of $erg\ s^{-1}\ cm^{-2}\ \text{Å}^{-1}$): $f_{excess} = f_{obs} - f_{cont}$

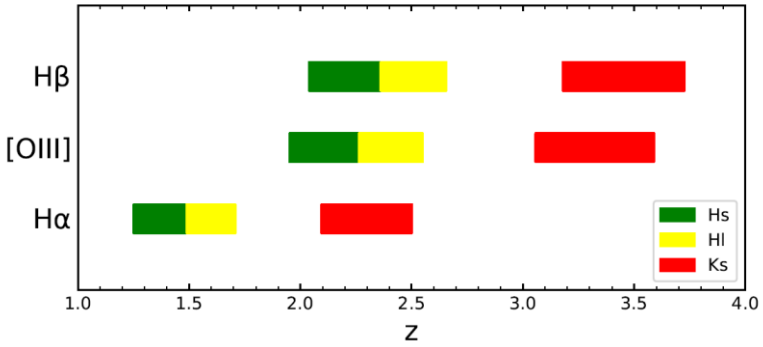

  - 2.2.1 SED fitting with emission line templates
    - The SED fittings sometimes overestimate continuum fluxes of the galaxies
    - Fitting and Assessment of Synthetic Templates (FAST)
    - W/O spectrum lines:

      The continuum levels can be significantly overestimated resulting in the overestimated stellar masses by at most ~ 0.8 dex

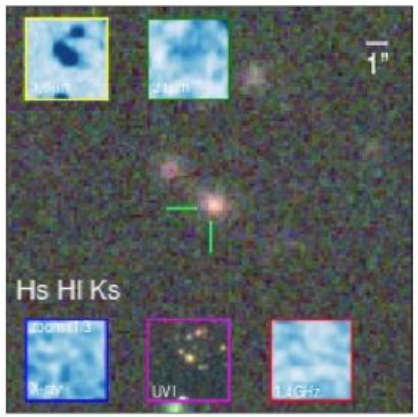
1"
Hs HI Ks
UVI

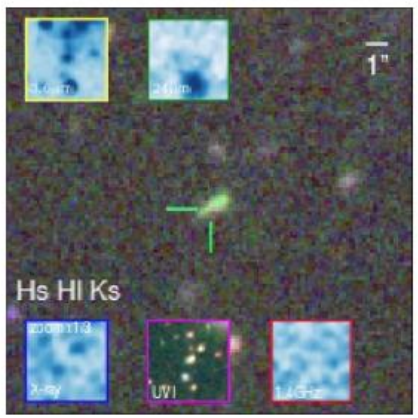
1"
Hs HI Ks
UVI

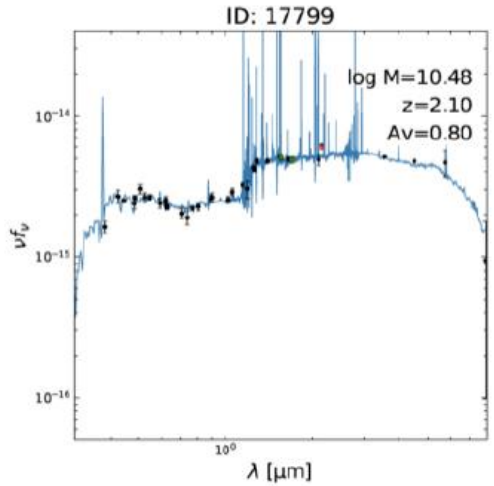
ID: 17799
log M=10.48
z=2.10
Av=0.80
νf_ν
λ [μm]

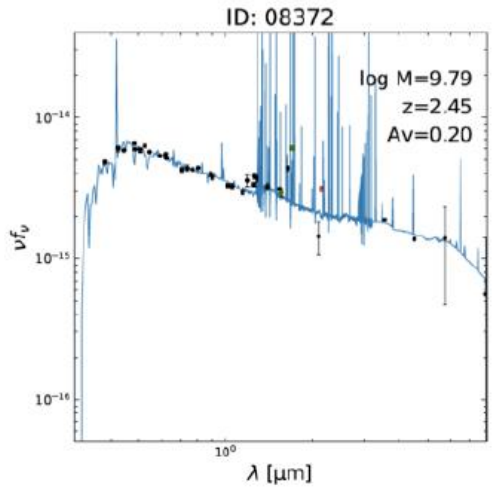
ID: 08372
log M=9.79
z=2.45
Av=0.20
νf_ν
λ [μm]

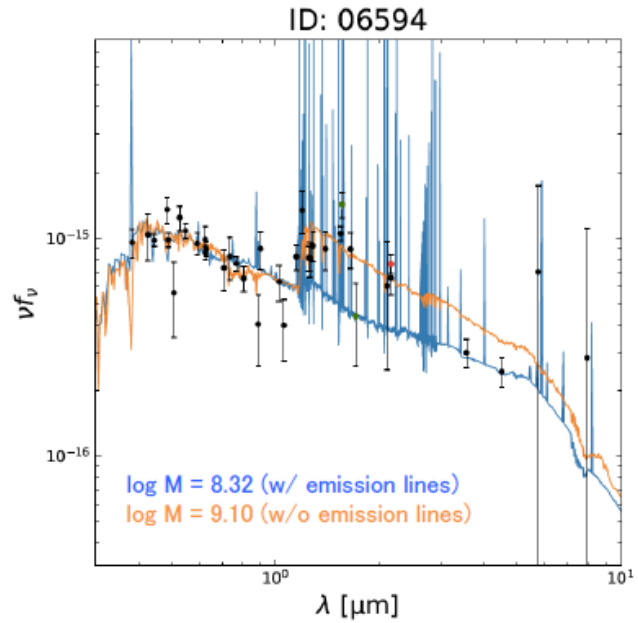
ID: 06594
log M = 8.32 (w/ emission lines)
log M = 9.10 (w/o emission lines)
νf_ν
λ [μm]

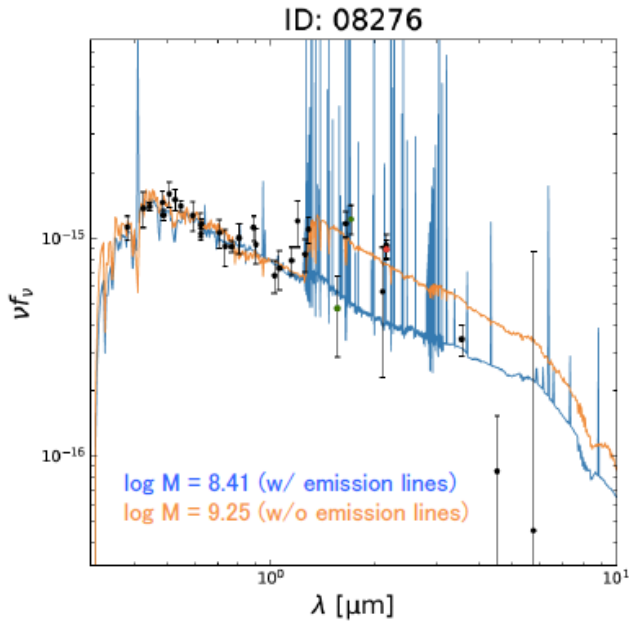
ID: 08276
log M = 8.41 (w/ emission lines)
log M = 9.25 (w/o emission lines)
νf_ν
λ [μm]

- 2.2.2 Robustness of the flux excess
  - The line strengths in the templates strongly depend on model assumptions. (Uncertainties)
  - The continuum fluxes estimated are more robust against the model assumptions.
  - The emission line fluxes derived from the flux excesses are more reliable than those derived from only the SED fitting

- 2.2.3 Selection of Hα emitter candidates at z = 2.1–2.5
  - The flux excesses in the Ks-band to be twice larger than its photometric errors
    → 2005 Hα emitters (699, 632, and 674 in COSMOS, UDS, and CDFS)
  - Hα fluxes (in units of $erg\ s^{-1}\ cm^{-2}$): $f_{\mathrm{H}\alpha} = r_{\mathrm{H}\alpha} \times f_{\mathrm{excess}} \times \Delta\lambda,$
    $r_{H\alpha} \sim 0.79$ (a ratio of Hα to total strengths of all emission lines), Δλ is Ks bandwidth

- 2.2.4 Selection of [OIII] emitter candidates at z = 2.1–2.5
  - 623 emitters in H_s band, 841 emitters in H_I band.
  - ([OIII]λ5007/Hβ) varies from 1 to 10 for typical star-forming galaxies at z ~ 2.3
  - Hα/Hβ = 2.8, and take dust attenuation into consideration ($A_{H\alpha}, \mathrm{A}_{\mathrm{H}\beta}$):

$$f_{\mathrm{H}\beta,\mathrm{obs}} = \frac{1}{2.8} \times 10^{0.4(\mathrm{A}_{\mathrm{H}\alpha} - \mathrm{A}_{\mathrm{H}\beta})} \times f_{\mathrm{H}\alpha,\mathrm{obs}},$$

  - $f_{total} - f_{H\beta,obs} = f_{O[III]}$, [OIII]λ5007/[OIII]λ4959 = 2.97 → f_{5007}

- 2.3 Flux comparisons with other methods
  - 2.3.1 Narrow-band imaging
    - NB209 filter: central wavelength 20,987 Å and a FWHM of 208 Å
    - Selection procedure in NB209: S/N > 5, color excesses with a > 3Σ significance, above lower limit
    - 86% (63/73) of the narrow-band selected galaxies are also selected by our method based on Ks-band excess.
    - 46/63 (73%) of the Hα emitters have consistent values within a factor of. σ = 0.16 dex.

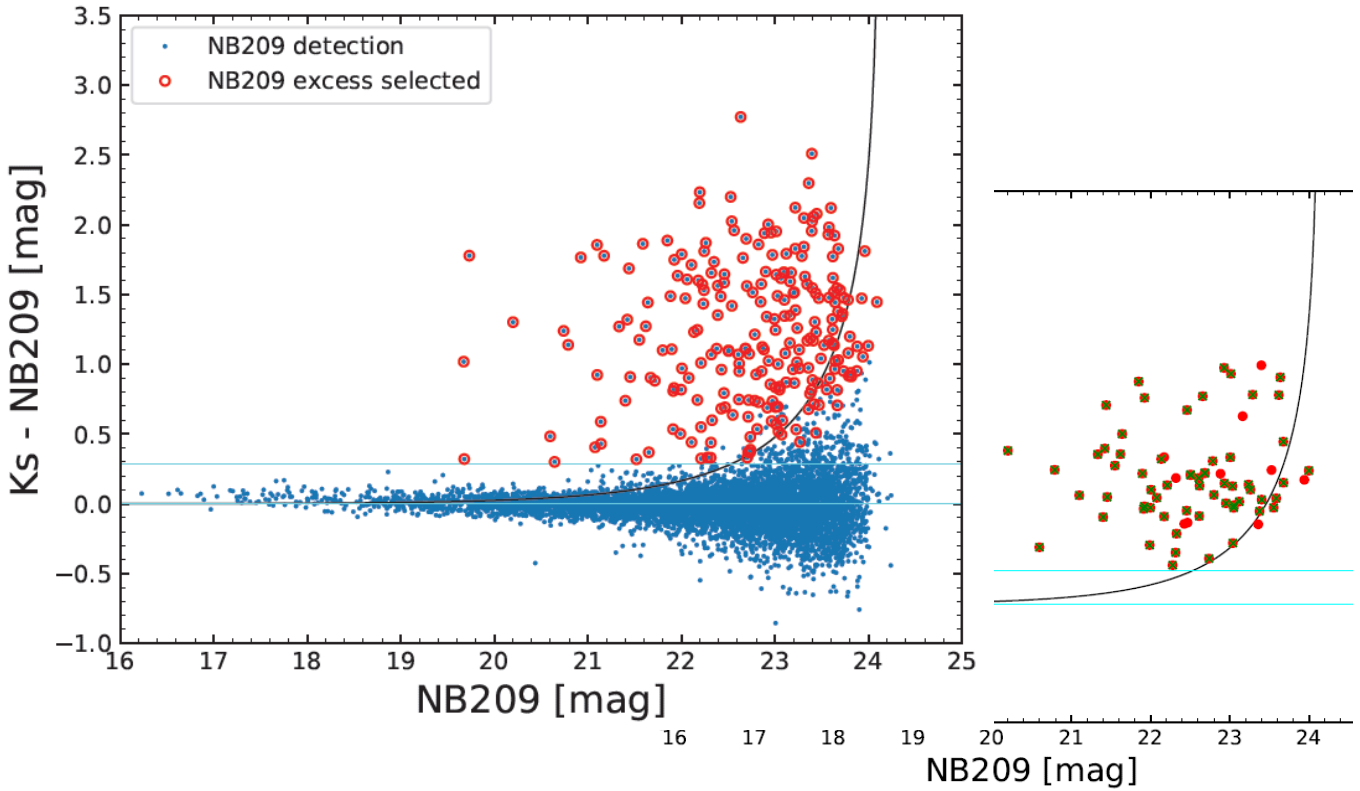

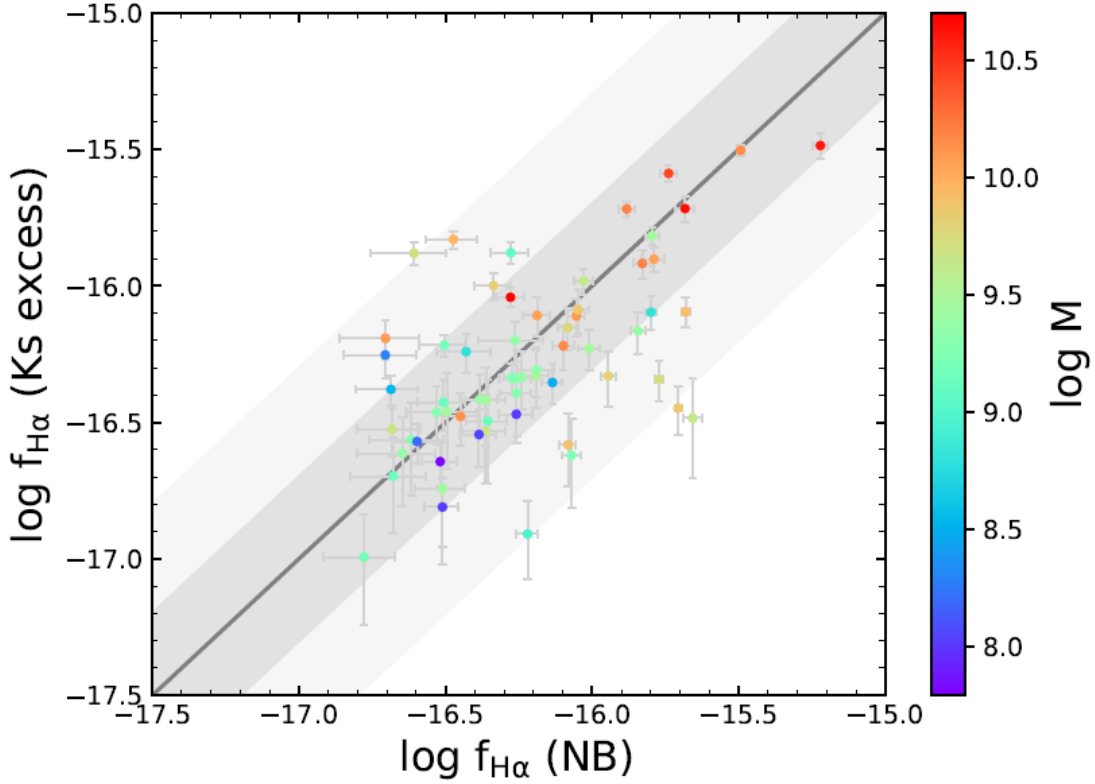

- 2.3.2 Long-slit spectroscopy
  - 93 Hα emitters in COSMOS have also been observed in ZFIRE.
  - Our values are higher than those of the ZFIRE with a median offset of 0.42 dex. (difference in aperture sizes and aperture corrections)
  - 62/93 (67%) of the Hα emitters have consistent fluxes within a factor of 2. σ = 0.21 dex.
- 2.3.3 Integral-field spectroscopy
  - KMOS3D: spatially resolved spectroscopic information on galaxies
  - 53/86 (62%) of the Hα emitters, the fluxes are consistent within a factor of 2. σ = 0.23 dex.

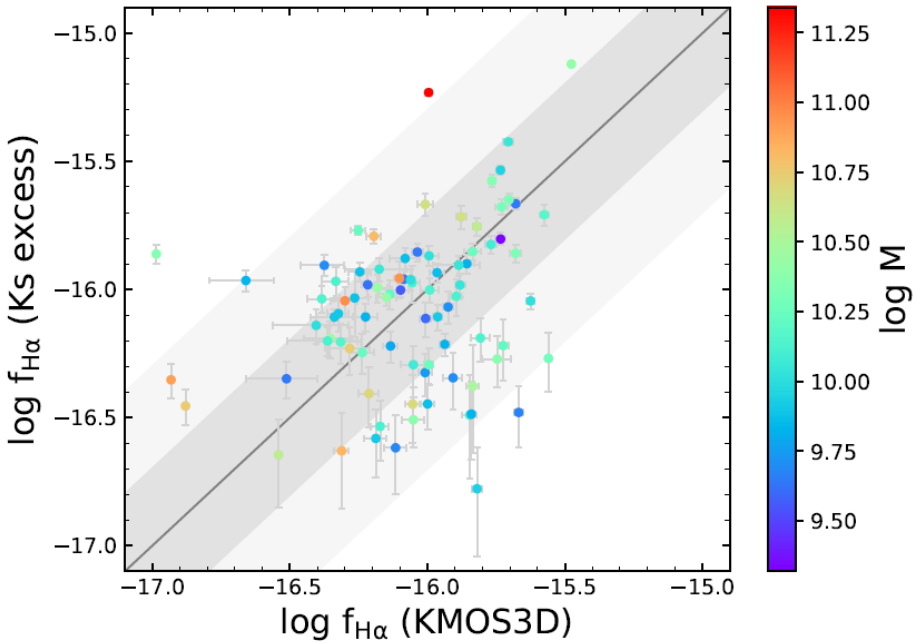

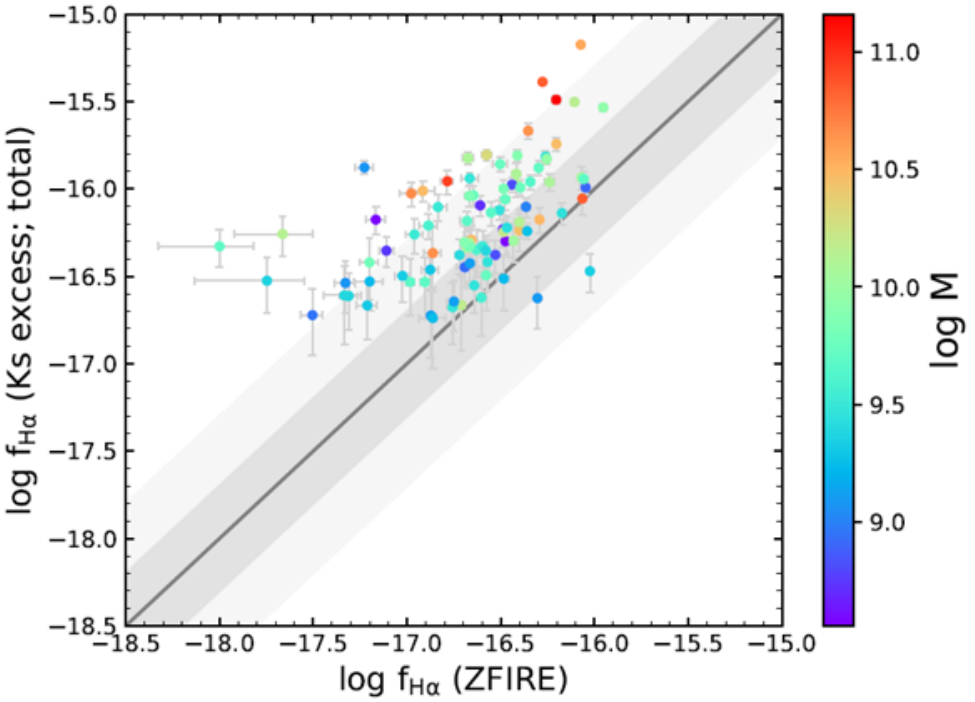

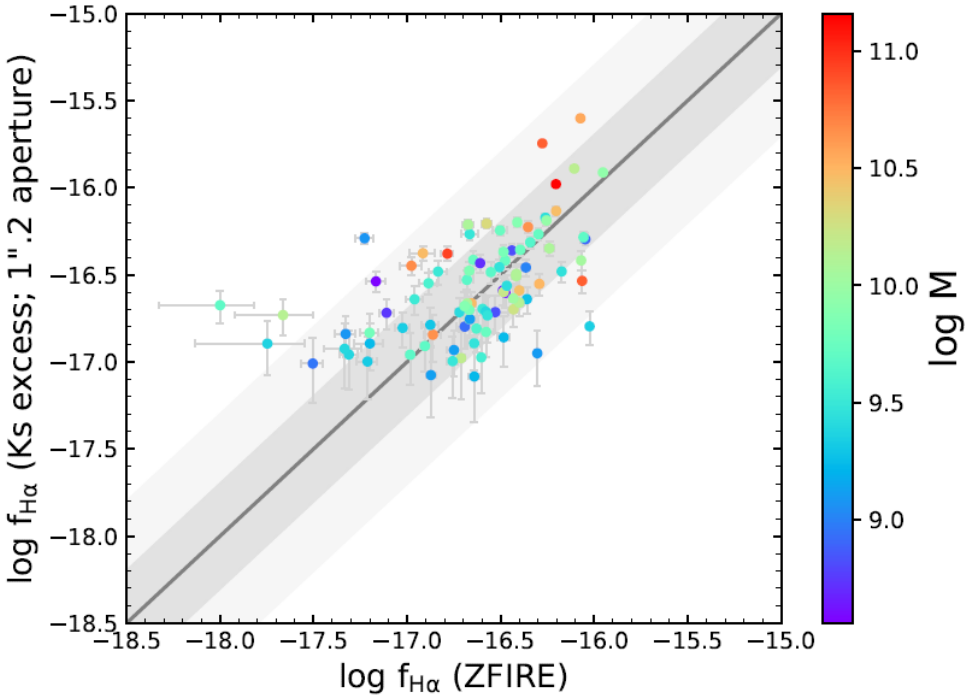

- 2.4 SFR and correction for dust extinction
  - 2.4.1 UV SFR (1216—3000 Å)
    - $L_{UV} = 1.5 v_{2800} L_{v,UV}$ (Bell et al. (2005))
    - $SFR(UV) = 1.09 \times 10^{-10} \times 2.2 L_{UV}$ (Fioc & Rocca-Volmerange (1997), assuming the Chabrier (2003) IMF)
  - 2.4.2 IR SFR (8—1000μm)
    - $SFR(IR) = 1.09 \times 10^{-10} \times L_{IR}$, where L_{IR} is the bolometric IR luminosity (Bell et al. (2005))
  - 2.4.3 Attenuation by dust
    - The dust attenuation at rest-frame 1600 Å **(IRX-method)**:

      $$A_{1600} = 2.5\ log\left[\frac{SFR(IR)}{SFR(UV)} + 1\right]$$ (Nordon et al. (2013))
    - A_{1600} is then converted to $\text{Å}_{H\alpha}$ according to the extinction curve of Calzetti et al.(2000). (f-factor = 1)
    - For galaxies with low S/N IR detection, estimate the dust attenuation from A_V derived by the FAST $\left(A_{V(FAST)}\right)$
    - Transfer FAST into IRX: $A_{V,\mathrm{IRX}} = 0.034 A_{V,\mathrm{FAST}}^3 - 0.230 A_{V,\mathrm{FAST}}^2 + 1.59 A_{V,\mathrm{FAST}}.$ Then, A_{IRX} to $A_{H\alpha}$. Calzetti et al.(2000).
  - 2.4.4 Hα luminosity and SFR
    - $L_{H\alpha} = f_{H\alpha} \times 4\pi d_L^2 \times 10^{0.4 A_{H\alpha}}$
    - $SFR(H_\alpha) = 7.9 \times 10^{-42} \times L_{H\alpha} \times 10^{-0.24}$ (Kennicutt (1998), assuming the Chabrier (2003) IMF)

Properties of Hα emitters at z = 2.1–2.5

- 3.1 Locations on the UVJ diagram
  - Most of the Hα emitters (by “flux excess”) are classified as the star-forming galaxies.

    (AGNs: red open circles)
  - 37 Hα emitters (1.8%) in the quiescent region.
    - SED for quiescent galaxies (22 of 37 galaxies have a 3σ excess)
    - Possibility of artificial result: massive galaxies with strong stellar continua
  - The UVJ based on the amounts of dust attenuation (A_V)

    A_V increase toward the upper right in the star-forming region

    Quiescent galaxies: indeed have small AV values.

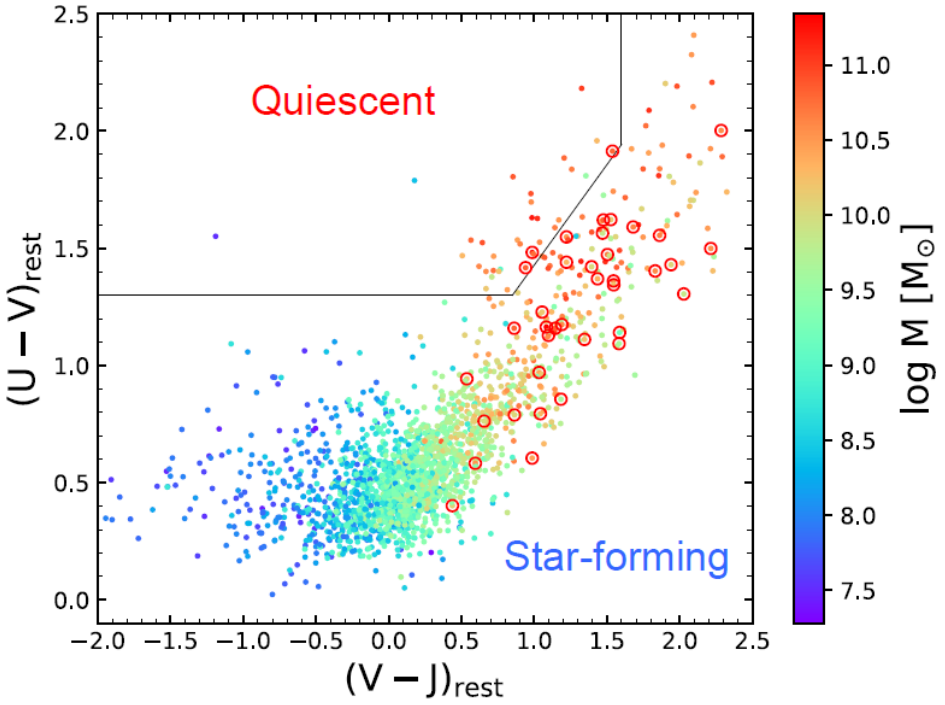

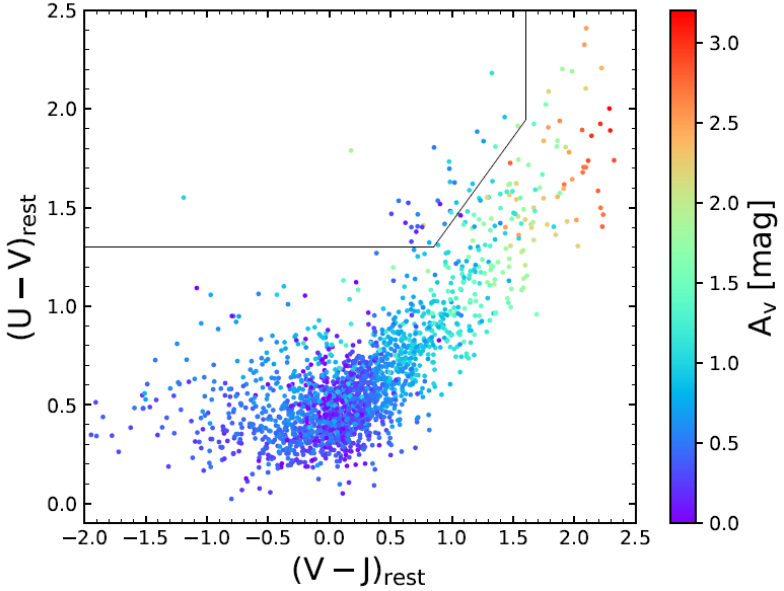

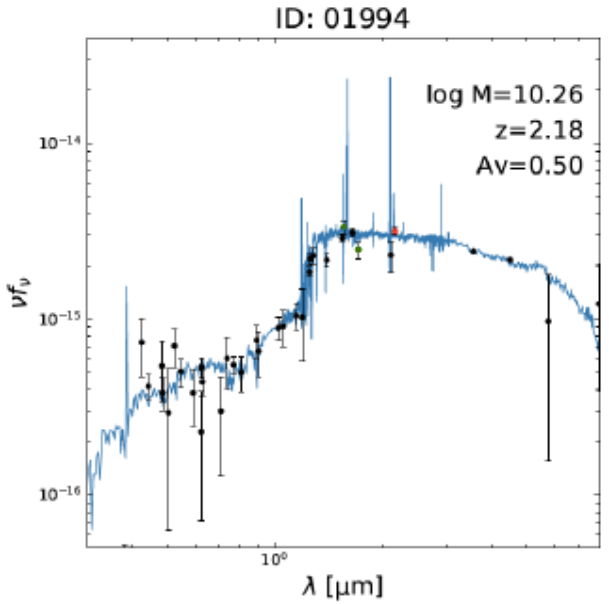

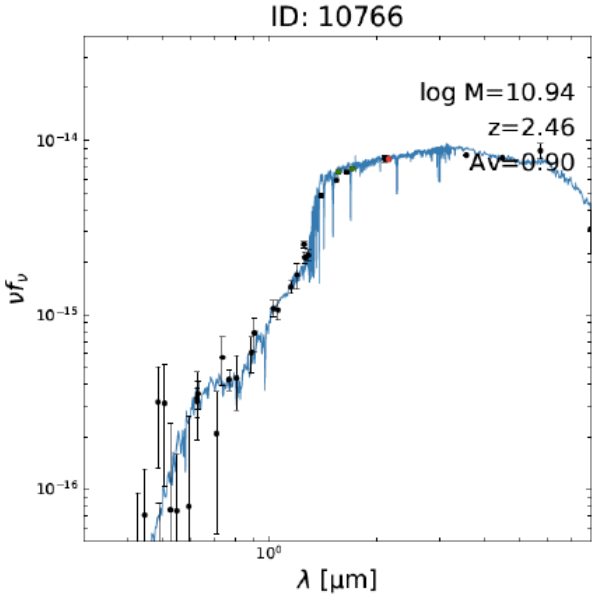

- The UVJ based on the age
  - less- obscured SFG (Blue (U − V) colors), have younger ages
  - Dusty star-forming galaxies ((U-V)>1.0) on the upper right region show both young and old ages, and show a bimodal distribution.
  - The younger galaxies have higher A_V values than the older ones.

  - Conclusion: 2 populations
  - One is the population evolving from the lower left to the upper right in the star-forming region.
  - The other population (Starburst galaxies) represents young dusty star-forming galaxies which can be even younger than the young unobscured population.

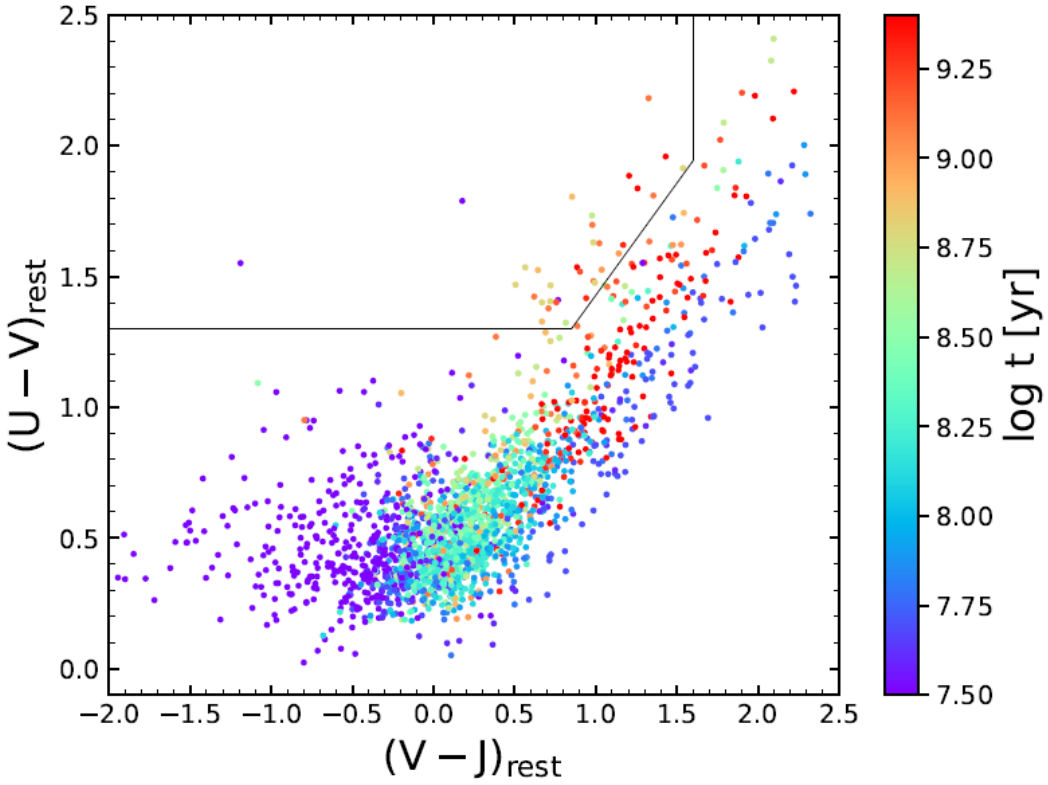

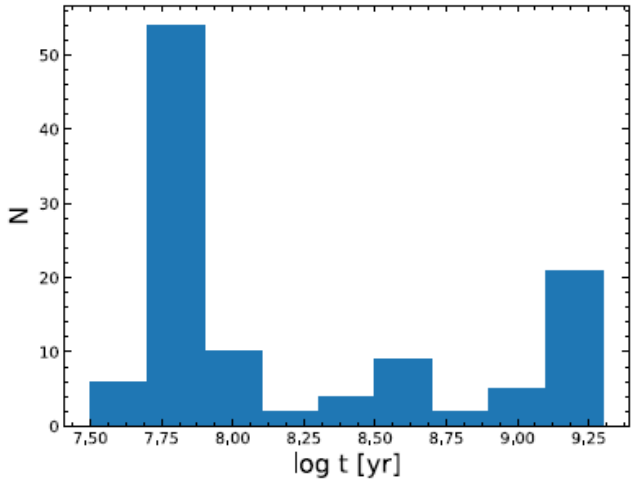

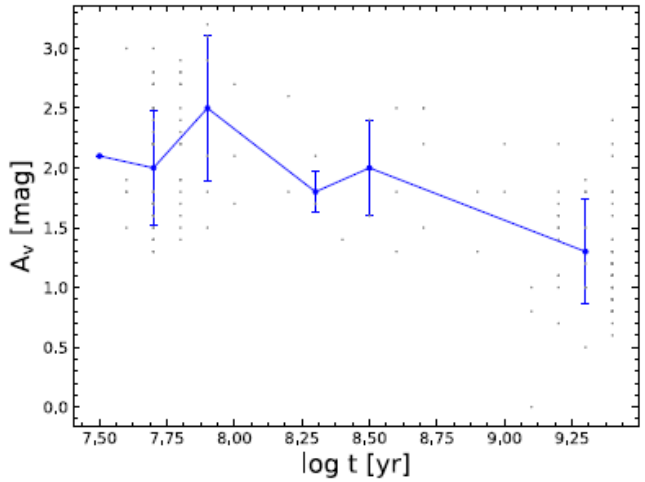

- 3.2 Equivalent width

$EW(all) = \frac{f_{excess}}{f_{cont}} \times W/(1+Z)$, W is the bandwidth of the Ks-band.

$EW(H_\alpha) = r_{H\alpha} \times EW(all)$, $r_{H\alpha} \sim 0.79$

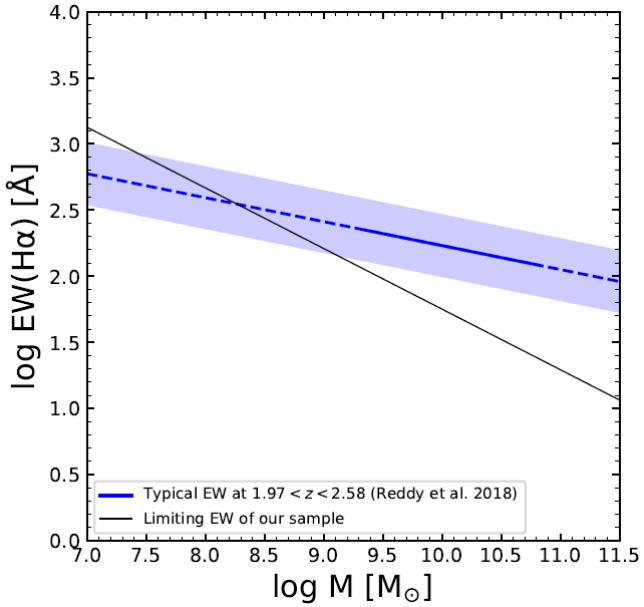

  - 3.2.1 Limiting equivalent width (photometric errors do not vary)

$$EW_{\rm min}({\rm H}\alpha) = r_{\rm H\alpha} \times \frac{2f_{\rm err}}{f_{\rm cont}} \times W/(1+z),$$

    - $EW_{min}(H_\alpha)$ is strongly correlate with the stellar masses: $\log EW_{\rm lim}({\rm H}\alpha) = -0.46 \log M + 6.33.$
    - Our sample is quite complete at log M > 9.0
    - The use of medium-band filters will increase the sensitivities to equivalent widths without losing the advantage of larger searching volumes compared to narrow-band filters.

  - 3.2.2 Stellar mass dependence
    - The Hα equivalent widths as a function of stellar mass:
      $logEW(H_\alpha) = -0.24\ logM + 4.54$
    - The fitting is done by $logM/M_\odot$ > 9.0
    - At low mass end, there are many low-mass Hα emitters with extremely high Hα equivalent widths (> 500 Å)

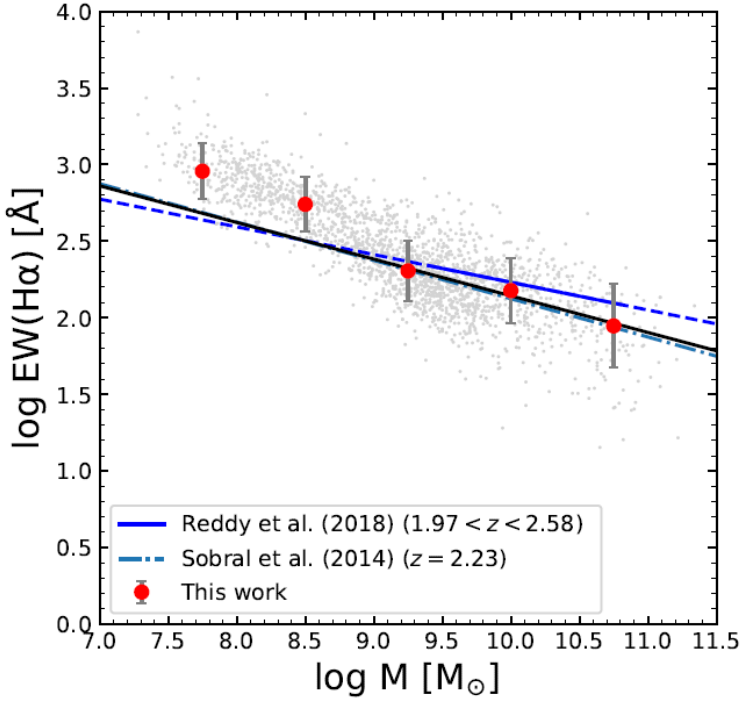

- 3.3 Dust attenuation
  - 3.3.1 Correlation between SFR and dust attenuation
    - The galaxies with higher SFRs should be more obscured by dust (produced by supernovae and AGB stars)
    - $A_{H\alpha} = 0.95\ logSFR(H_\alpha) - 0.51,$
    - $A_{H\alpha} = 0.99\ logSFR(UV + IR) - 0.61$
  - 3.3.2 Different extinctions between IRX and SED fitting
    - There is an offset between the amounts of the attenuation derived from the IRX and the SED fitting by the FAST. (IRX is ~ 0.21 mag larger than SED fitting)
    - SED fitting based on UV continua are easily affected by the interstellar dust.
    - However, the IRX method directly measures the ratios of the absorptions and re-radiations.
    - Therefore the IRX can better trace the total amounts of the dust attenuation than the SED fitting.

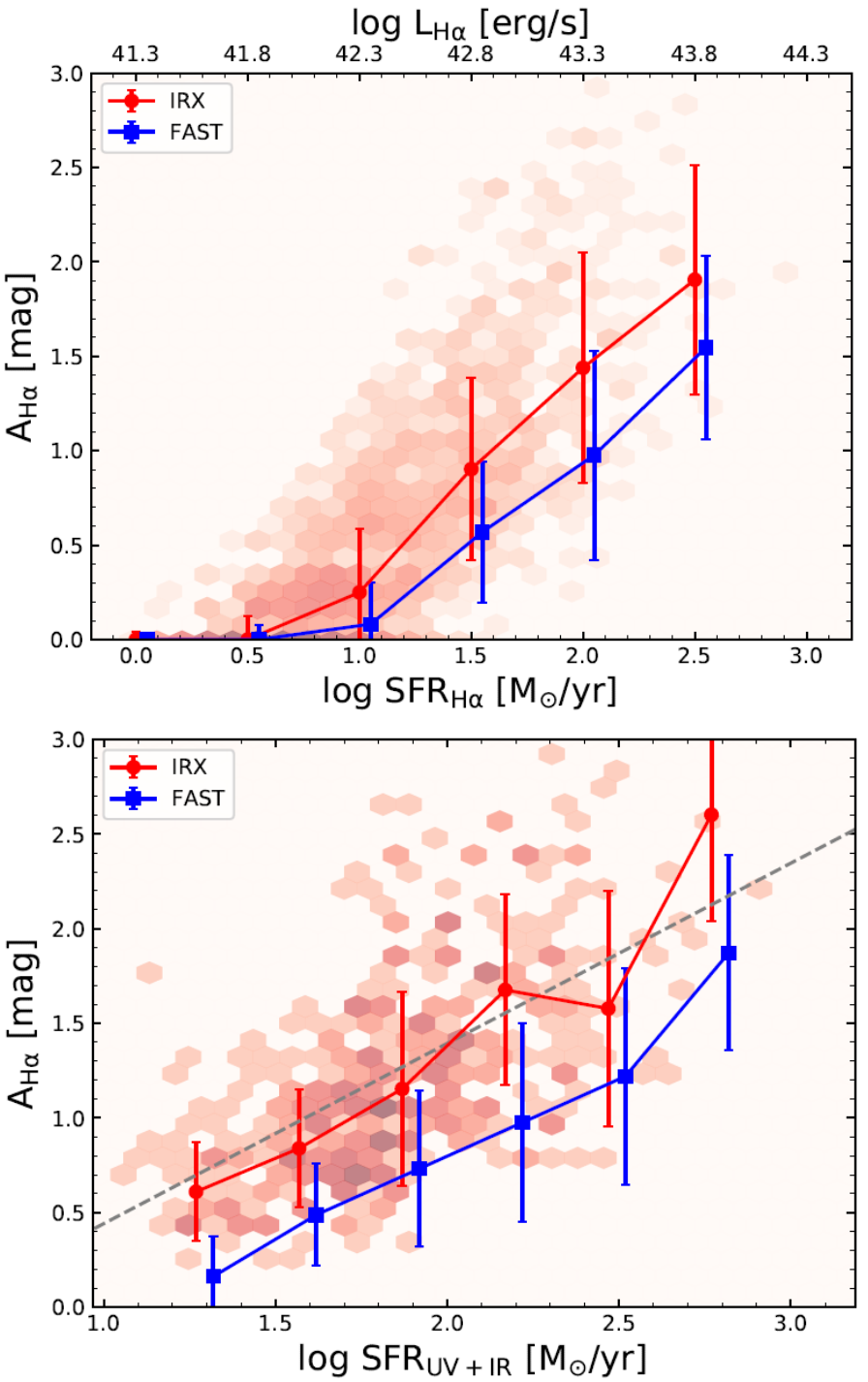

Figure 3.8: Correlation between Hα SFRs (luminosities) and the amounts of the dust attenuation to the Hα emission lines, $A_{H\alpha}$. The red hexagonal tiles show the $A_{H\alpha}$ distribution of our sample, where $A_{H\alpha}$ values are derived by the IRX as described in § 2.4.3. Median values of $A_{H\alpha}$ in SFR bins derived from the IRX and the SED fitting by the FAST are shown in the red circles and the blue squares, respectively.

- 3.4 Hα luminosity function

  Comparison with the result of a narrow-band imaging survey: HiZELS

  - 3.4.1 Completeness estimate
    - The Hα luminosity completeness of the sample: 100,000 mock galaxies.
    - Calculating fractions of the emitters above the detection limit.

Table 3.1: Simulated completeness in Hα luminosity bins

$\log L(\mathrm{H}\alpha)$ (erg/s)	< 41.25	41.5	41.75	42.0	42.25	> 43.0
completeness (%)	0	1.4	35	85	96	100

    - Almost all the galaxies with log L(Hα) > 42.25 are selected as the emitters and no need for correction.
  - 3.4.2 Calculation
    - 3.4.2.1 Number density
    - The comoving volume: ΔV ~ $5.51 \times 10^5\ Mpc^3$
    - The width of the luminosity bins: Δ(log L) = 0.25
    - The number density:

$$\phi(\log(L_c)) = \frac{1}{\Delta(\log L)} \sum_{|\log \frac{L_i}{L_c}| < \frac{\Delta \log L}{2}} \frac{1}{\Delta V},$$

    - 3.4.2.2 Schechter function fitting

$$\phi(L)dL = \ln 10 \phi^* \left(\frac{L}{L^*}\right)^{\alpha} e^{-(L/L^*)} \left(\frac{L}{L^*}\right) d\log L,$$

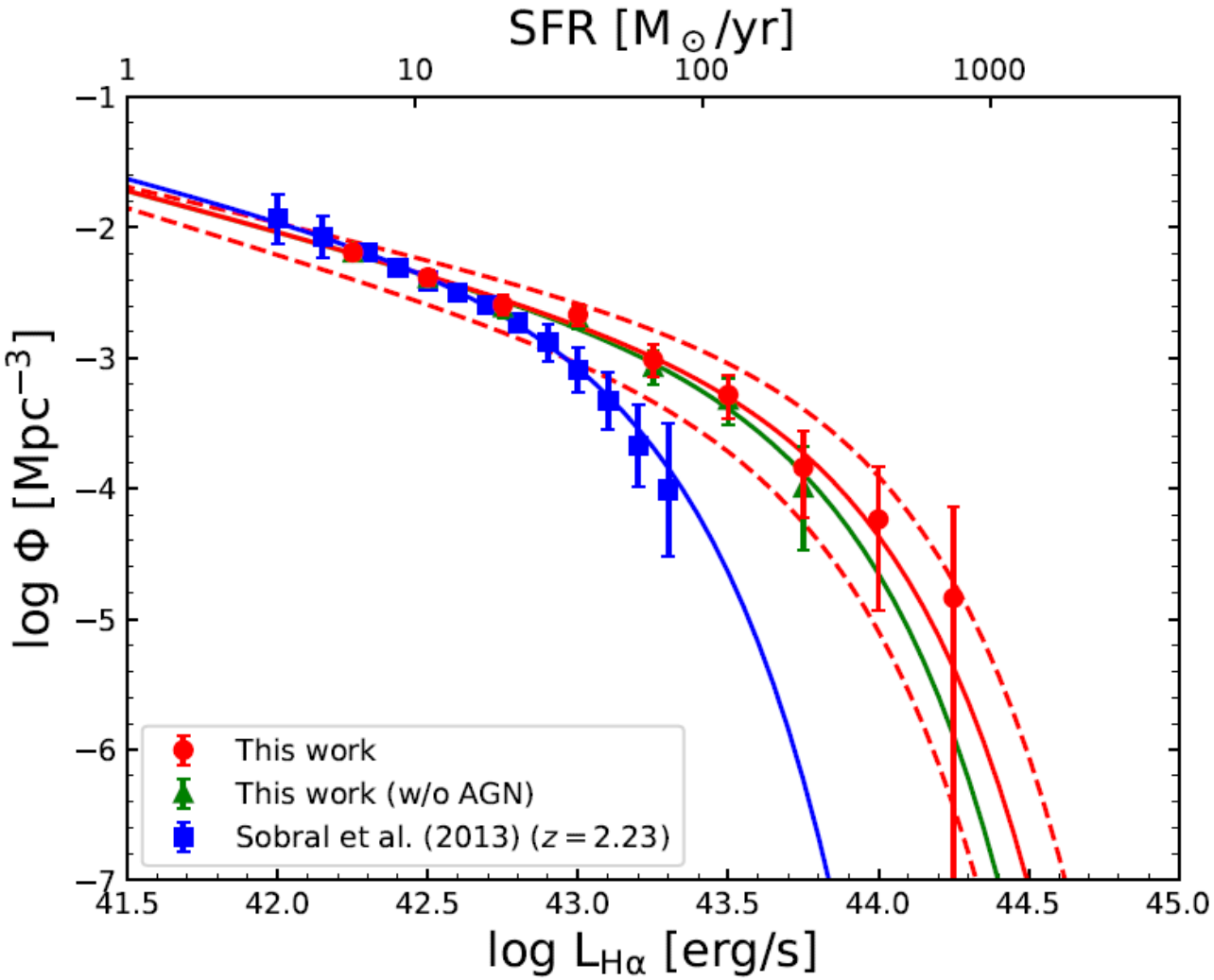

Table 3.3: Best-fit parameters of Hα luminosity functions

	α	$\log L^*$	$\log \phi^*$
This work	-1.62	43.6	-3.38
This work (w/o AGN)	-1.61	43.5	-3.30
This work ($A_{\mathrm{H}\alpha} = 1$)	-1.53	43.3	-3.11
Sobral et al. (2013)	-1.59	42.9	-2.78
Sobral et al. (2013) w/ correction	-1.74	43.2	-3.09

- There is an excess in the bright-end of our luminosity function compared to that of Sobral et al.(2013), while the faint-end slopes are consistent.

- 3.4.3 What causes the bright-end excess?

  Two possible causes: One is related to structural properties of the galaxies,

  Another is the different corrections for the dust extinction

  - 3.4.3.1 Extended Hα profile
  - Radial profiles of Hα emission lines are more extended than stellar components

    → The sizes of apertures (HiZELS: fixed 2″ aperture) may miss some fractions of the Hα fluxes)

Cumulative fractions of Hα:

$$I(R) = I_e \left\{ -b_n \left[\left(\frac{R}{R_e} - 1 \right)^{1/n} \right] \right\}, \quad \Gamma(2n) = 2\gamma(2n, b_n),$$

Table 3.4: Structural parameters of Nelson et al. (2016)

$\log M/M_\odot$	n	R_e (kpc)
$9.0 < \log M/M_\odot < 9.5$	1.83 ± 0.15	1.77 ± 0.11
$9.5 < \log M/M_\odot < 10.0$	1.98 ± 0.16	2.91 ± 0.17
$10.0 < \log M/M_\odot < 10.5$	1.47 ± 0.10	3.10 ± 0.20
$10.5 < \log M/M_\odot < 11.0$	1.90 ± 0.20	5.34 ± 0.80

- The radius corresponding to the 2″ aperture at z = 2.23 is ~ 8 kpc. (seeing ~ 1”)
- In the bright-end of the luminosity function, Sobral et al. (2013) might have missed ~ 40% of the Hα fluxes.

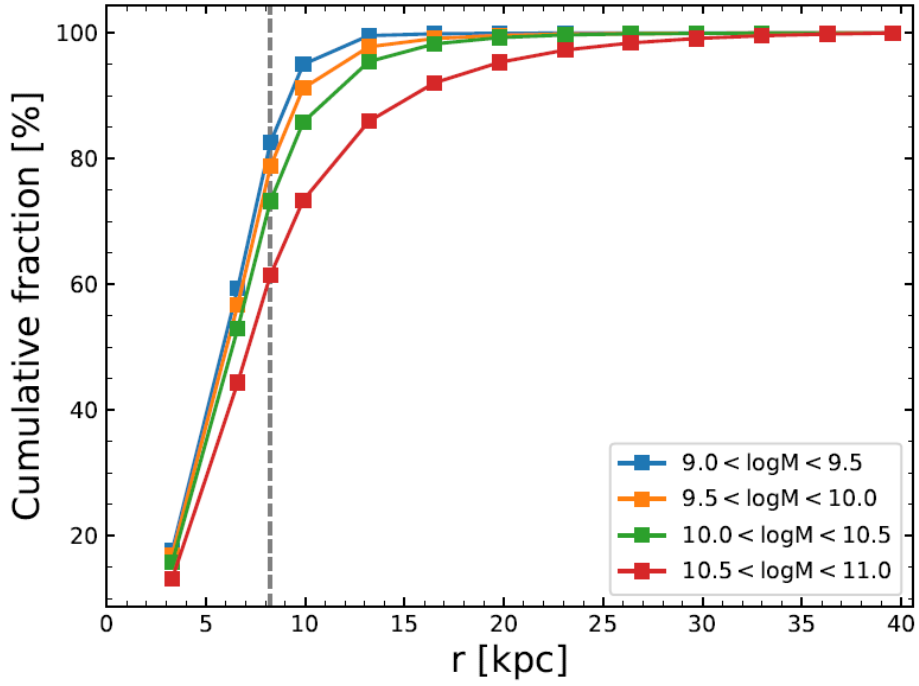

Figure 3.12: Cumulative fractions of Hα as a function of radius in our simulation. They are obtained assuming the Sérsic profiles with the structural parameters of Nelson et al. (2016) and the seeing of the HiZELS observation. The color coding reflects stellar masses of the galaxies, while the grey vertical dashed line shows the physical scale corresponding to the 2″ aperture used in Sobral et al. (2013).

PSF corresponding to the seeing: $$\mathrm{PSF}(r) = \frac{\beta - 1}{\pi^2 \alpha} \left[1 + \left(\frac{r}{\alpha}\right)^2\right]^{-\beta},$$

The FWHM of the seeing, β=2.5: $$\mathrm{FWHM} = 2\alpha\sqrt{2^{1/\beta} - 1}.$$

- After correction, about half of the excess in our luminosity function can be explained by the missing Hα fluxes in Sobral et al. (2013).

- 3.4.3.2 Strong attenuation to the luminous galaxies
  - The manner of the correction for the dust attenuation
  - Sobral et al. (2013) have assumed $A_{H\alpha}$ = 1 mag for all the galaxies
  - This research: $A_{H\alpha} = 0.95\ logSFR(H_\alpha) — 0.51$
  - Sobral et al. (2013) underestimated intrinsic luminosities of the brightest Hα emitters.

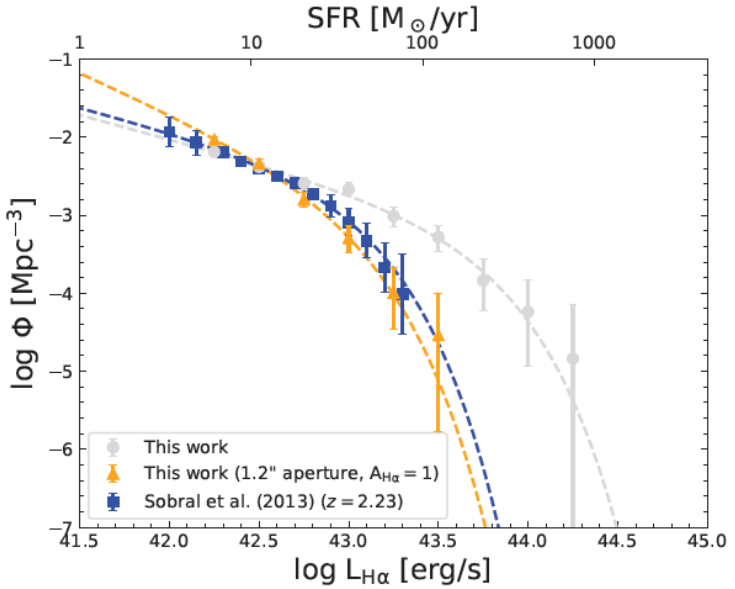

Figure 3.13: Hα luminosity function derived from the ZFOURGE data without the aperture corrections assuming $A_{H\alpha} = 1$ (orange triangles). The difference between this work (grey circles) and Sobral et al. (2013) (blue squares) is almost completely reduced.

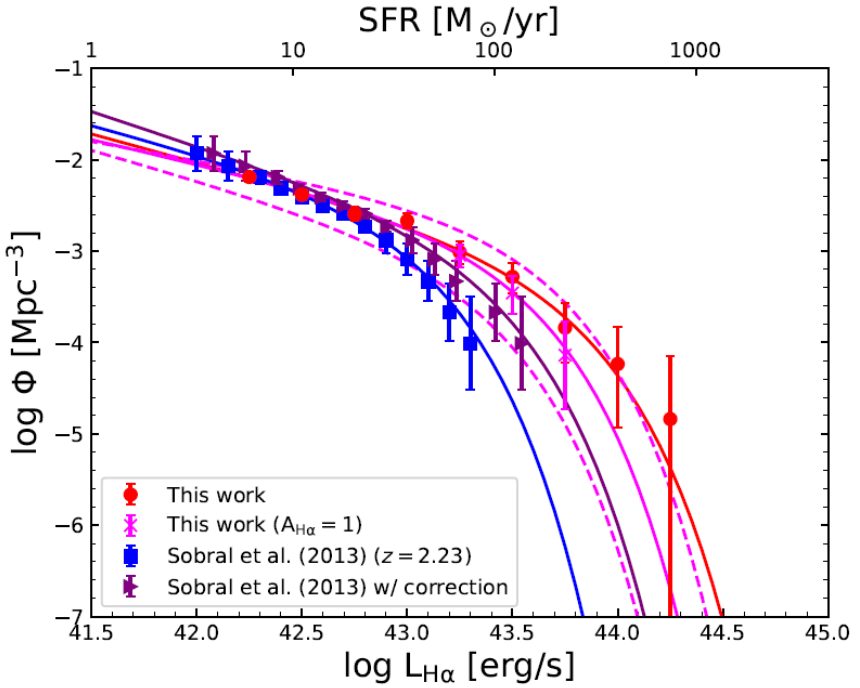

- 3.4.4 Cosmic star formation rate density
  - By integrating the luminosity function, we can derive a cosmic SFRD at $2.1 < z < 2.5$.

    (Excluding AGN, 13% of total Hα luminosity)

  - Our SFRD agrees well with those observations and the Hα emitter selection successfully reproduces the entire populations of star-forming galaxies.

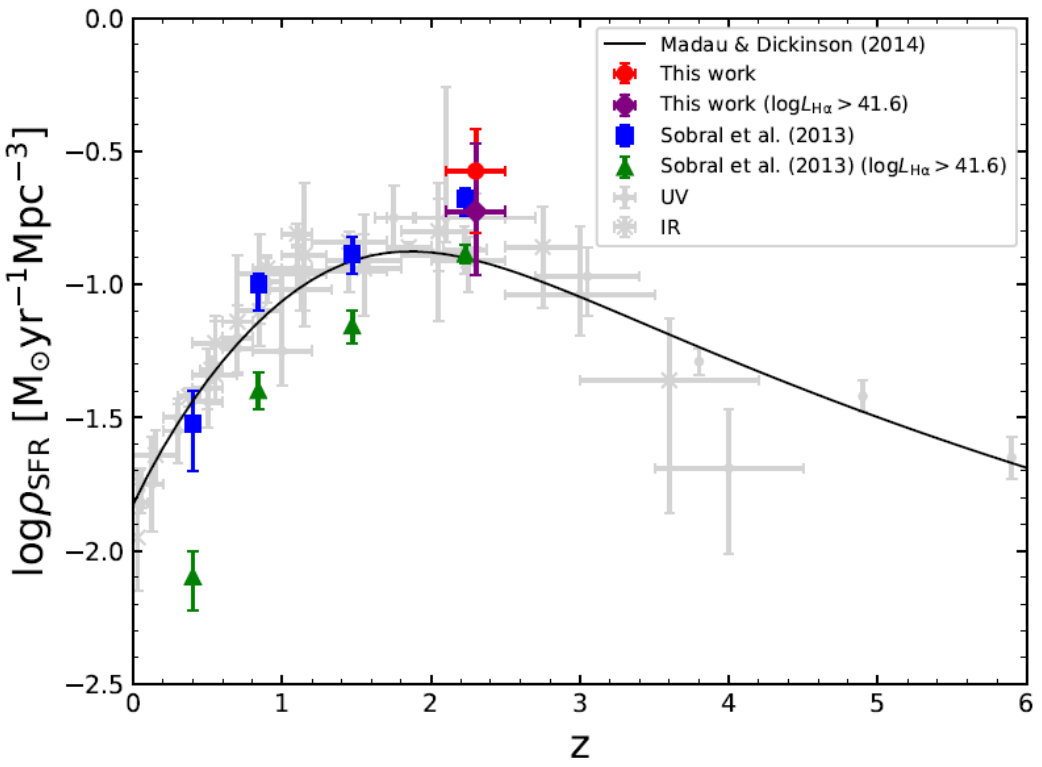

Figure 3.16: Our cosmic star formation rate density in the context of its redshift evolution reported by previous studies. The red circle and blue squares represent our measurement and the results of Sobral et al. (2013), respectively, which are obtained by integrating the Hα luminosity functions. AGN contributions have been removed from both values. The grey circles and crosses show the results of previous studies summarized in Madau & Dickinson (2014) for a comparison, which are measured from UV and/or IR luminosities.

- 3.5 Star formation main sequence
  - All the AGNs identified by either X-ray, IR, or radio (38/2005) are removed while the quiescent Hα emitters are included.

  - 3.5.1 Main sequence at z = 2.1–2.5

Fitting result: $\log SFR(H_\alpha) = 0.66\, logM - 5.32$
(Mass range: $9 < logM/M_\odot < 11$)

    - Good agreement with (Whitaker et al. 2014), where SFRs were derived from UV+IR luminosities
    - The small offset in the most massive bins, is probably due to different selections for the star-forming galaxies. (Bias: dusty starburst systems)
    - However, Hα emitters represent a less-biased population.

(At Mass ~ 11, the offset of this research is caused by quiescent Hα emitters ?)

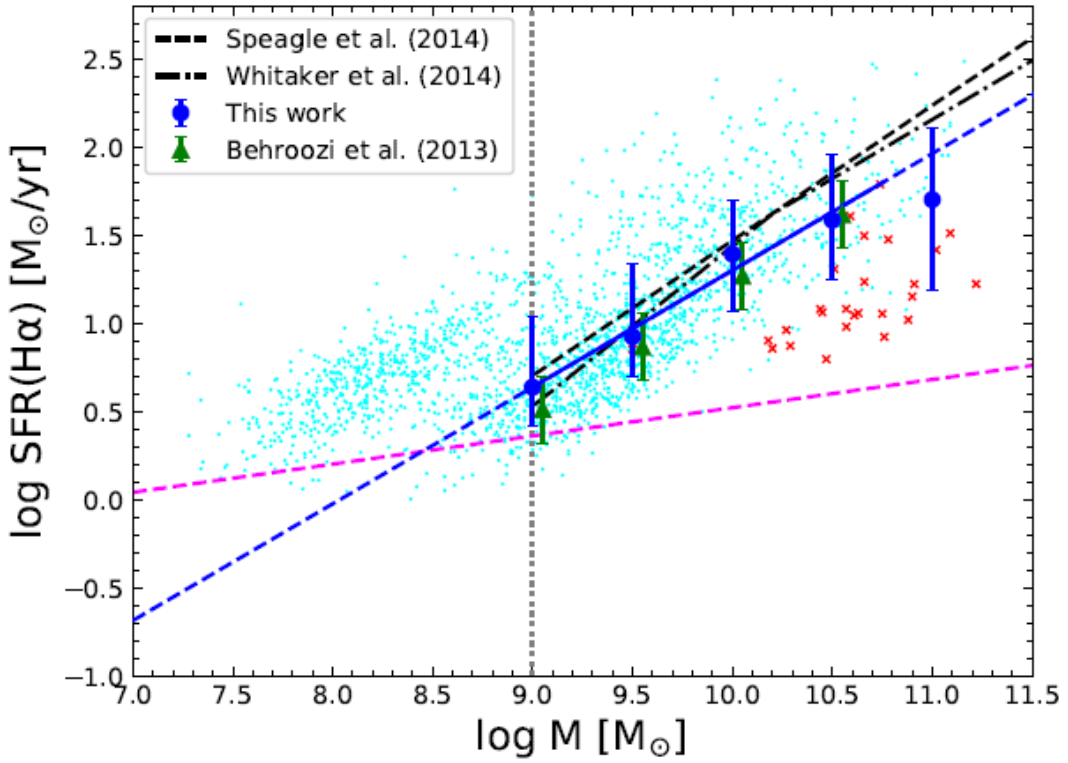

Figure 3.17: Hα star formation main sequence (SFMS) of our sample. The cyan circles represent individual galaxies while the blue circles show median values in each stellar mass bin. By fitting in the range of $9 < \log M < 11$, we obtain the best-fit SFMS shown by the blue line. The green triangles are the typical values among many previous studies with various wavelengths, which are summarized in Behroozi et al. (2013). The black dashed and dash-dotted lines indicate the best-fit SFMSs of Speagle et al. (2014) and Whitaker et al. (2014), respectively. The red crosses represent the quiescent Hα emitters with well-constrained SEDs classified by the UVJ diagram. The dotted grey vertical line shows the stellar mass completeness limit of our sample while the dashed magenta line is the SFR limit of our sample corresponding to the flux excess threshold to be selected as the Hα emitters.

- 3.5.2 Low-mass galaxies with high sSFR
  - At $logM/M_{\odot} < 9$, there are many low-mass galaxies with much higher SFRs than predicted from the extrapolation of the SFMS.
  - Evaluating impacts of the photometric errors in the data on the sSFRs of the low-mass galaxies (100000 mock galaxies)
  - The $\gtrsim 0.5$ dex in SFMS can be hardly caused by only the errors
  - Conclusion: The low-mass galaxies with the high sSFRs are really starburst galaxies.

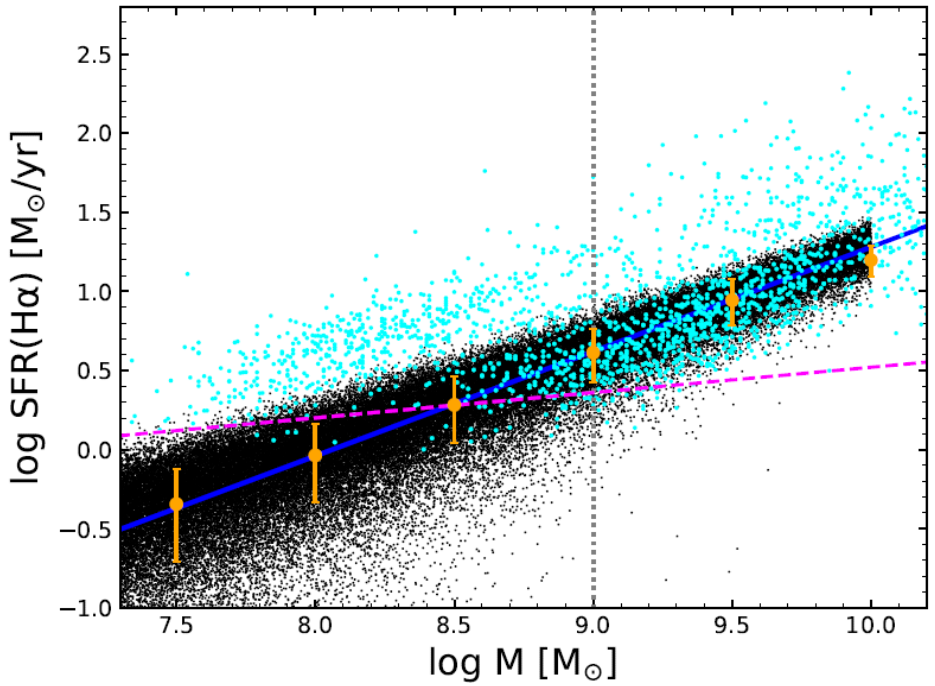

- 3.5.3 Hα/UV ratio
  - Instantaneous starburst: luminosity ratio between Hα and UV is expected to be different (Hα/UV ratio is higher)
  - The low-mass Hα emitters with high sSFRs we discovered are the galaxies which recently have experienced short period starbursts.

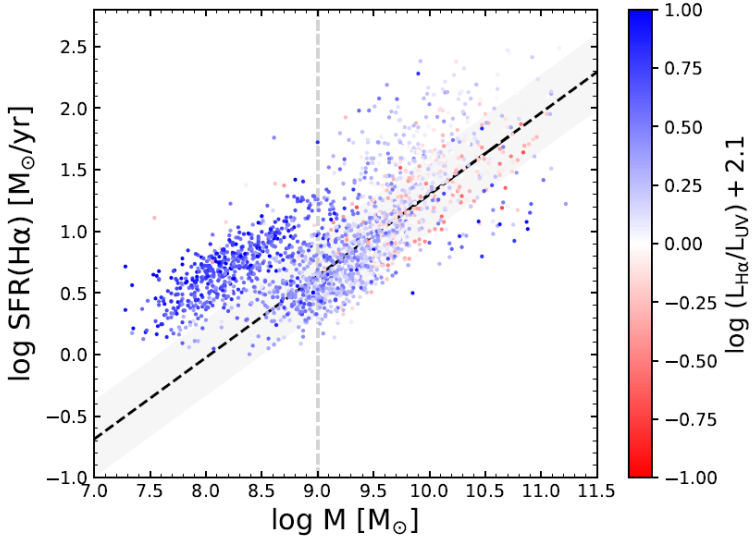

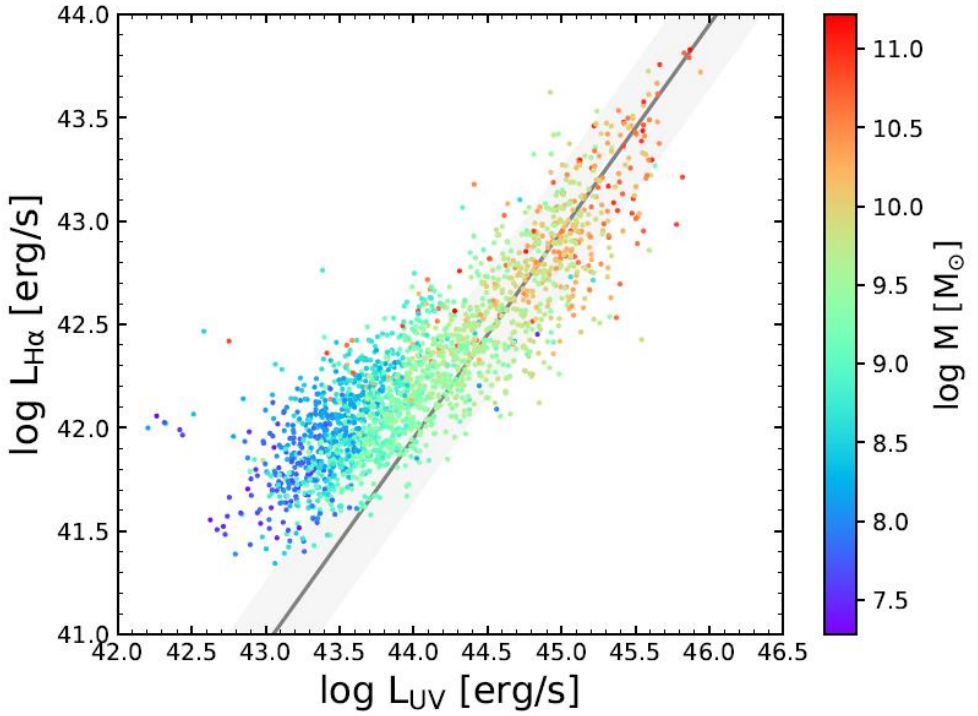

- 3.5.4 SFHs of the starburst galaxies
  - High-mass galaxies with high sSFRs, their Hα/UV ratios do not seem high

  → Starburst galaxies with different stellar masses have different SFHs (Different mechanisms)
  - Definition: Starburst galaxies: galaxies with SFRs above the SFMS by 0.3 dex.
  - At least two different types of the starburst:
  - 1. A burst with a short duration (lower mass) → high Hα/UV ratios
  - 2. A burst with a longer duration (higher mass)→ constant SFHs during > 10 Myr
  - Dominant mechanisms of the starbursts can vary with stellar masses of the galaxies.

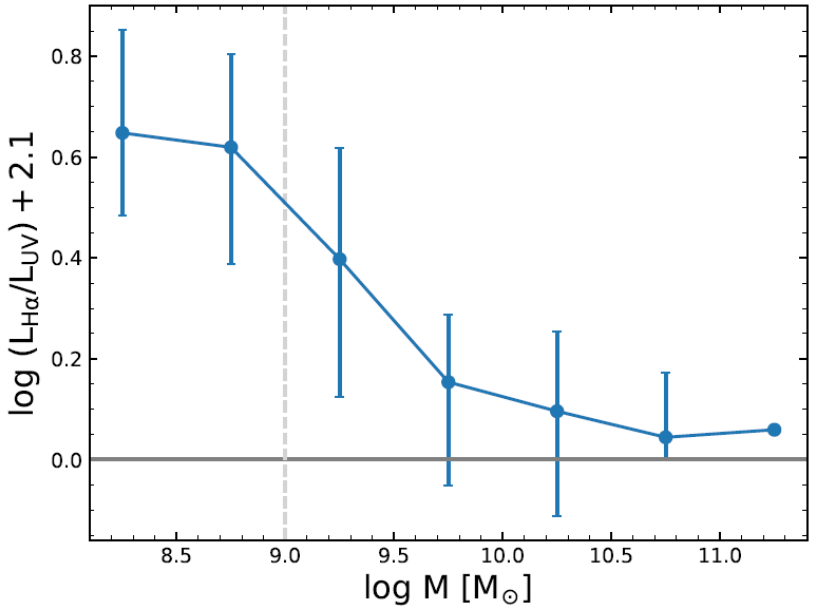

Figure 3.21: Hα/UV ratios of the starburst galaxies as a function of stellar mass. The blue circles represent median values in each stellar mass bin. The grey horizontal line shows the value expected from a constant SFH, while the dashed vertical line indicates the stellar mass completeness limit.

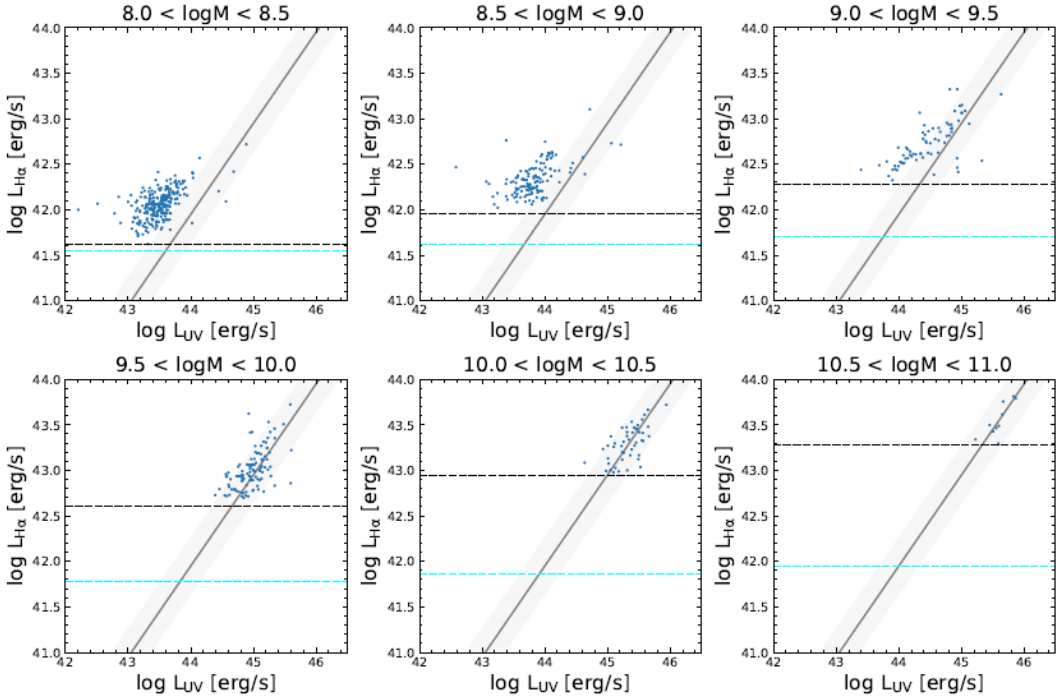

Properties of [OIII] emitters at z = 2.1–2.5

The galaxies with H_S/H_I excesses are [OIII](+Hβ) emitters
The strong [OIII] emitters represent a unique population characterized by low stellar masses, low metallicities, high sSFRs, and high ionization parameters.
The most extreme [OIII] emitters have also been related to large escape fractions of the ionizing photons.

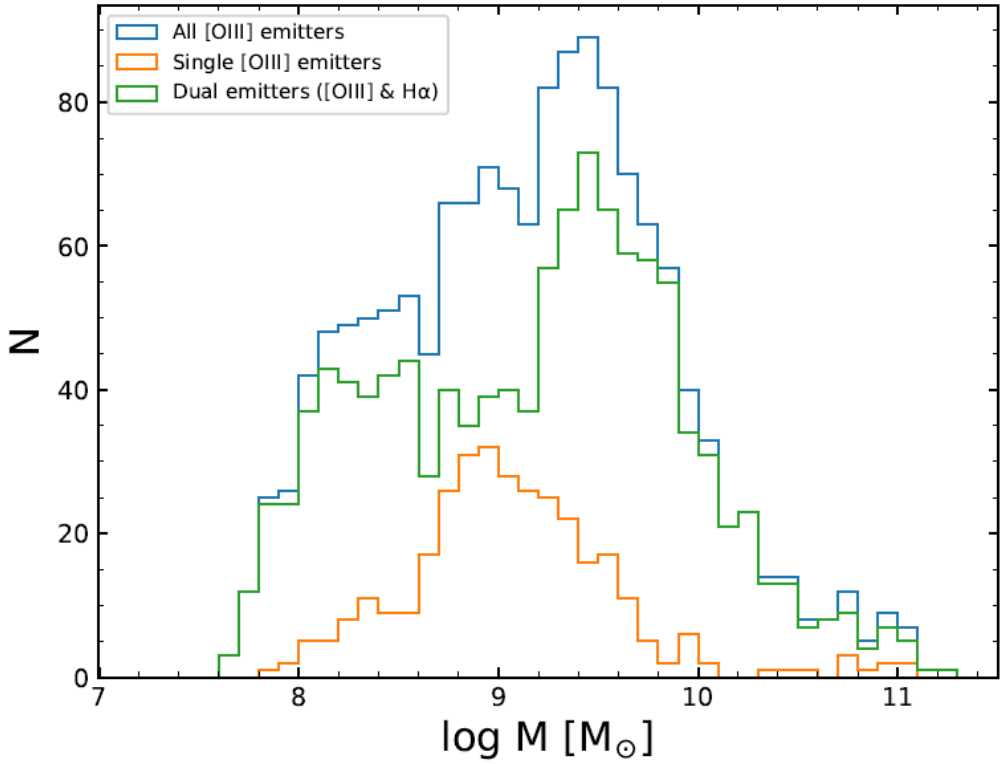

- 4.1 Sample description
  - 623 emitters in H_S band, 841 emitters in H_I band.
  - 1137 (78%) [OIII] emitters have been also selected as the Hα emitters. (dual emitters)
  - The discrepancy between the two distributions at $logM/M_{\odot} \sim 9$: **(Bimodality in dual emitters)**
    - 10% for photo-z uncertainties
    - The equivalent width completeness of Hα strongly depends on stellar, while the stellar mass dependence of the [OIII] equivalent width is more moderate. (Peak in the right)
    - Many lowest-mass ($logM/M\_\odot$ < 8.5) galaxies with extremely large Hα equivalent widths. (Peak in the left)
  - 357 emitters (2.26 < z < 2.36), Hβ and [OIII] fall into different filters
    - Corrected for median [OIII]/Hβ of ~ 5.4

- 4.2 Equivalent widths
  - 4.2.1 Limiting equivalent widths

$$\log EW_{\rm lim}([{\rm OIII}]+{\rm H}\beta) = -0.52\log M/M_{\odot} + 6.97.$$

    - The completeness is larger than 85% at $logM/M_{\odot}$ > 9

  - 4.2.2 Stellar mass dependence
    - The Hα equivalent widths as a function of stellar mass:
      $logEW([OIII]+H_{\beta}) = -0.42\ logM + 6.39$
    - For dual emitters (Hβ are estimated from the dust-corrected Hα luminosities)
      $logEW([OIII]) = -0.44\ logM + 6.46$
    - This suggests that the flux excesses in the H_s/H_I -band are dominated by the [OIII] emission lines.
    - The [OIII] equivalent widths depend on the stellar masses more strongly than those of Hα
    - The median equivalent widths of our [OIII] emitters agree well with an extrapolation of the best-fit relation even in $logM/M_{\odot}$ < 9.

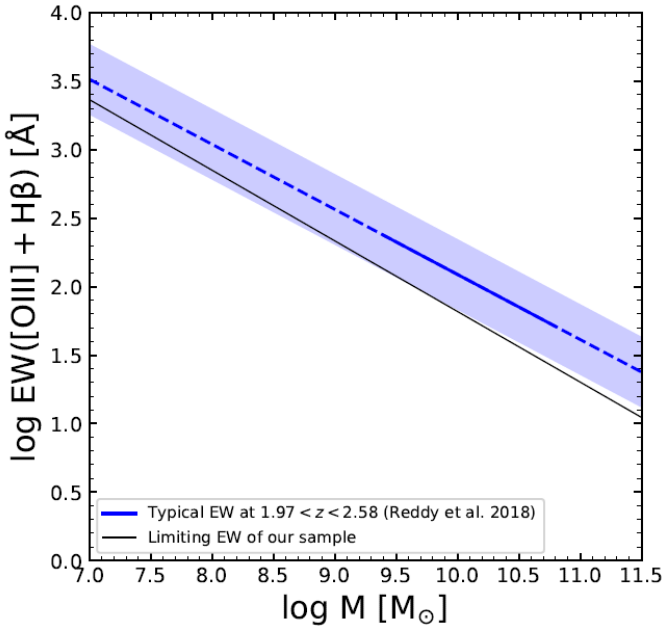

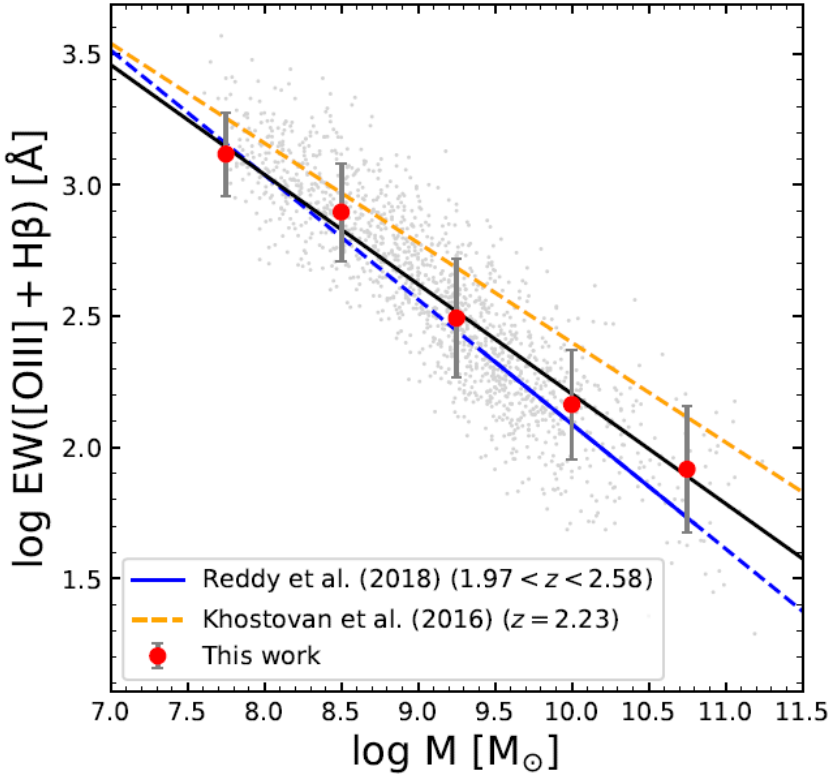

- 4.3 Correlation of [OIII] with other properties
  - 4.3.1 Hα sSFR
    - $logM/M_{\odot}$ > 9.0 fitting:

      $logsSFR(H_{\alpha}) = 0.67\ logEW([OIII] + H_{\beta}) - 10.0$

      - The low-mass galaxies with the highest sSFRs also show the largest [OIII] equivalent widths.

  - 4.3.2 [OIII]/Hβ

    $\log([OIII]\lambda5007/H_{\beta}) = 0.39\ logEW([OIII] + H_{\beta}) - 0.45$

    - [OIII]λ5007/Hβ ratios increase with the [OIII]+Hβ equivalent widths.

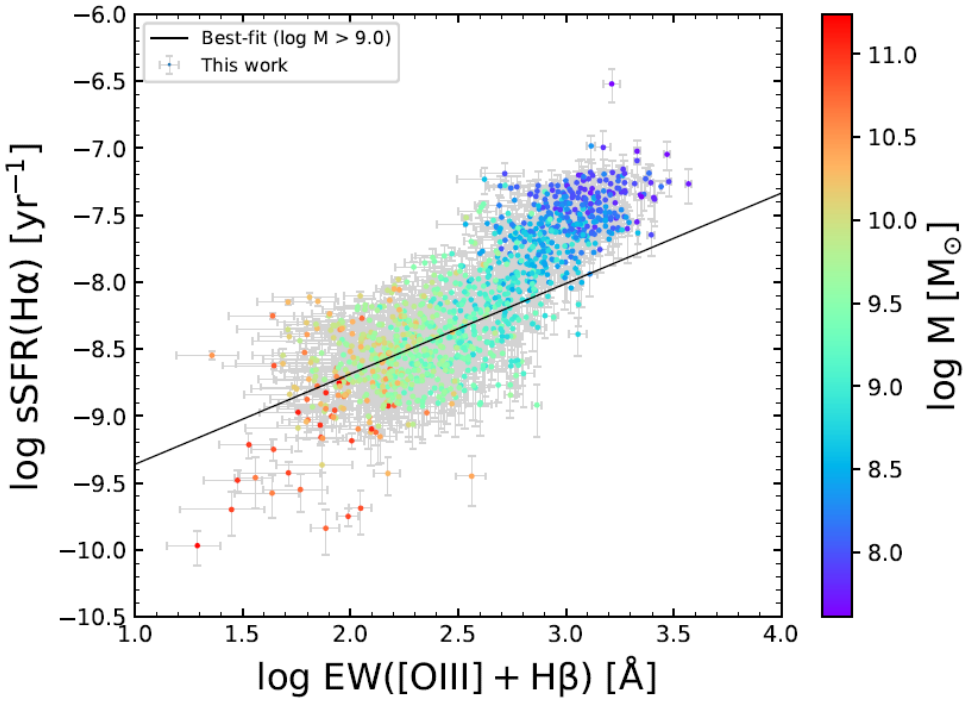

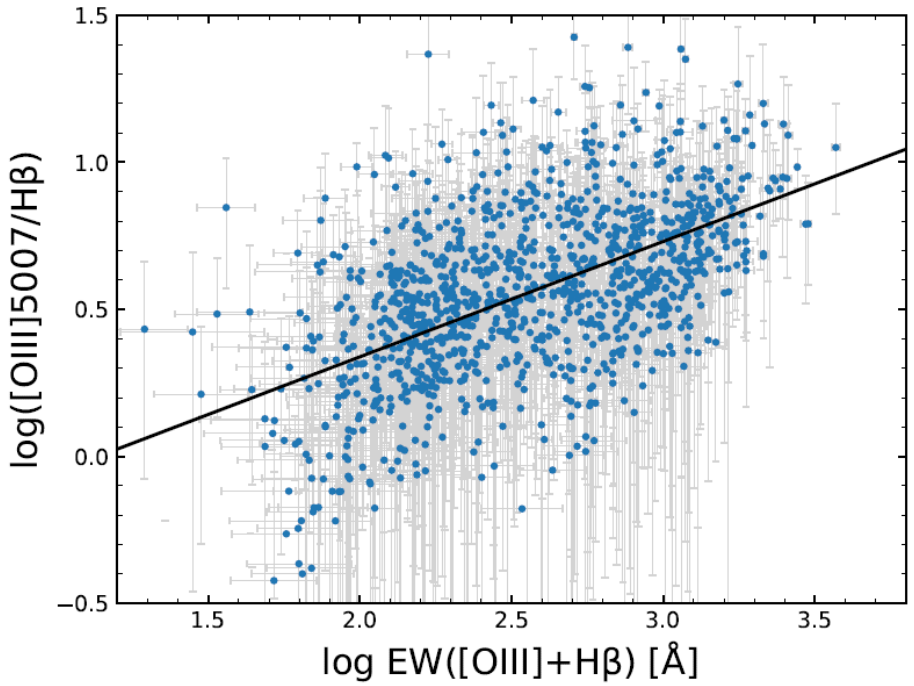

- 4.3.3 Dust attenuation
  - The stronger [OIII] emitters are less obscured by the dust.
  - The dust attenuation correlates with the SFR (§3.3)
  - The lower mass galaxies have lower SFRs (not sSFRs) compared to the more massive ones.
- 4.3.4 Ionization parameter
  - The low-mass galaxies with the highest [OIII] equivalent widths are expected to have large ionization parameters, which is due to the different stellar mass dependences of [OII] and [OIII]
  - [OII] equivalent widths do not significantly vary with stellar mass. (-0.171)
  - [OIII] equivalent widths depend much strongly on the stellar masses.(-0.42)
  - Large [OIII]/[OII] ratios are one of characteristics of the local galaxies with large escape fractions
- 4.3.5 Hα luminosity
  - Bowman et al. (2019) have found a good correlation between UV SFRs and [OIII] luminosities in the range of SFR $\sim 0-100\ M_{\odot}\ yr^{-1}$.
  - → Examining a relation between Hα SFRs and [OIII] luminosities (dual emitters)

$$\log L([OIII]) = 0.62 \log SFR(H\alpha) + 42.0, \pm 0.16 \text{ dex}$$

  - Tight correlation: galaxies in a certain SFR bin show similar metallicity values.
  - The slope is less than unity: massive stars producing ionizing photons but their production efficiencies are decreased.

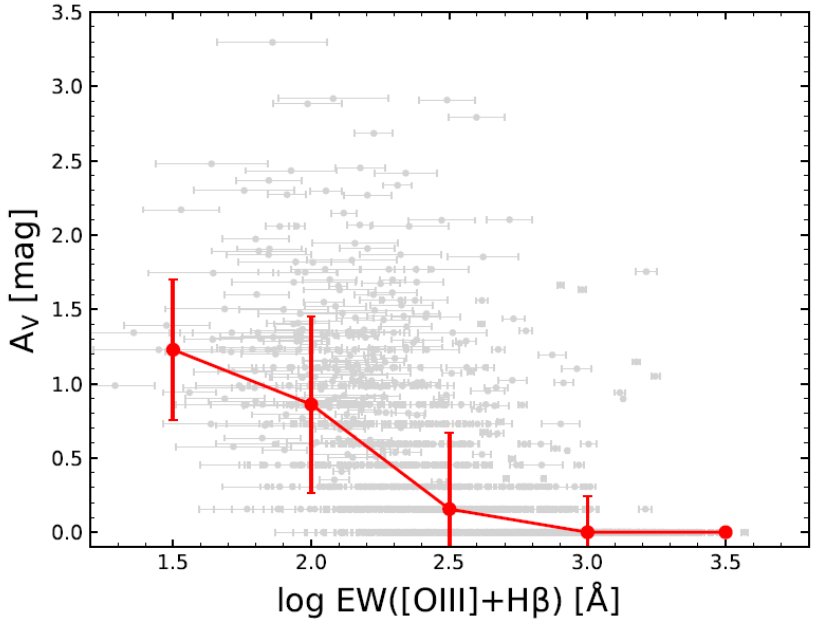

Figure 4.7: The amount of the dust attenuation (A_V) as a function of [OIII] + Hβ equivalent width for the dual emitters. The grey circles represent individual galaxies while median values in each bin are shown in red.

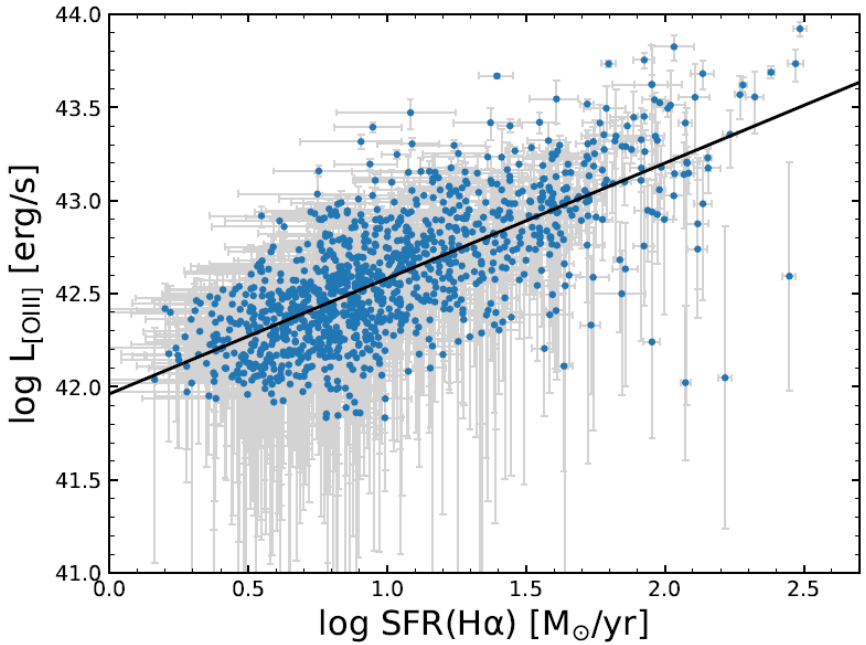

- 4.4 Overlap with the Hα emitters
  - Guess: The [OIII] emitters as a sub-population of the Hα emitters
  - 4.4.1 Distributions of properties
    - The stellar mass distributions: the three sub-populations are different from each other.
    - The Hα sSFR distributions of the dual emitters and the single Hα emitters: p ~ 0.0004. The peak on the right is more remarkable for the dual emitters.

    → The [OIII] strengths increase with the sSFRs
    - The distributions of the Hα equivalent widths (a proxy of sSFR): p ~ 0.85. The contributions of massive galaxies in the high equivalent width end.

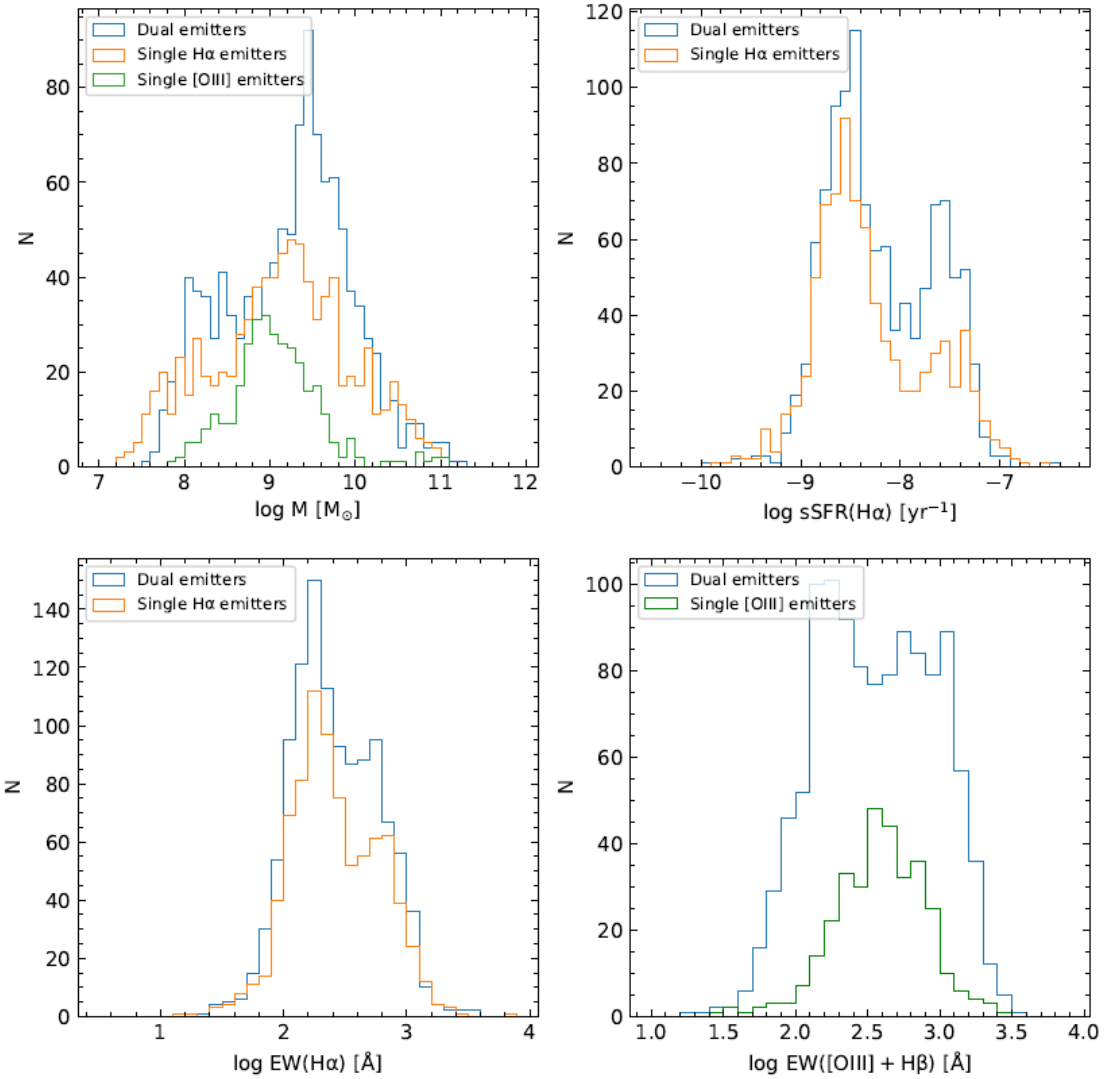

- 4.4.2 Dual emitter fraction
- Dual emitter fractions: Ratios of the numbers of the dual emitters to the total as a function of stellar mass
  - The dual emitter fractions of the [OIII] emitters are higher than 70% in all the bins suggesting that they represent a sub-population of the Hα emitters

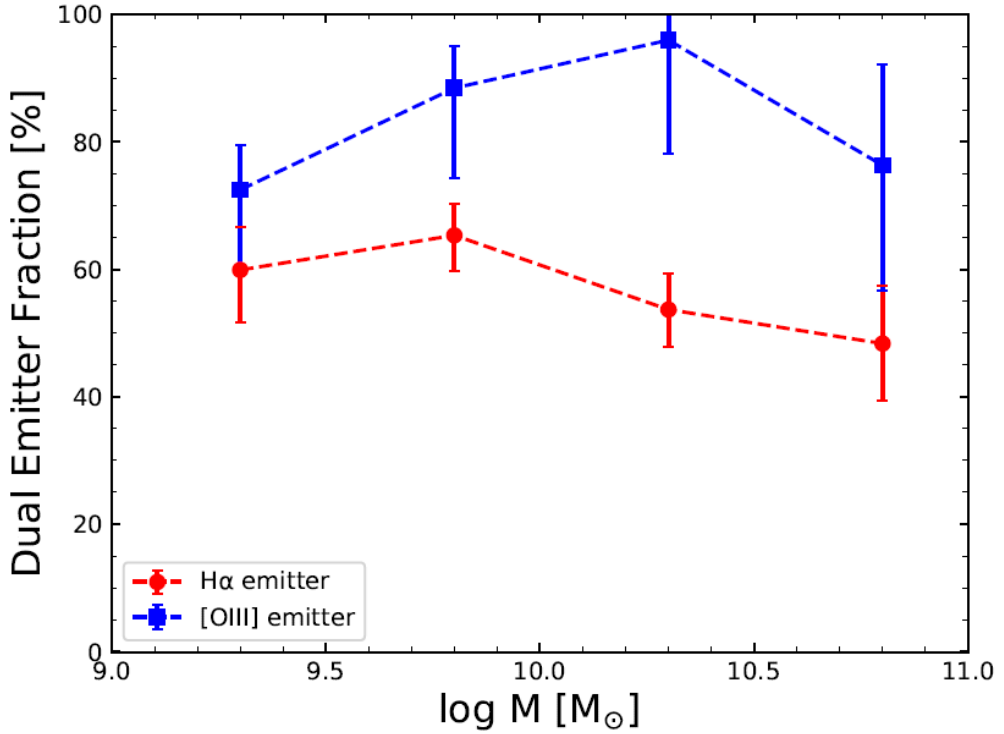

Figure 4.10: Dual emitter fractions as functions of stellar mass for both the Hα emitters (red) and the [OIII] emitters (blue). Each errorbar includes poisson and the uncertainties due to equivalent width sensitivities of our method.